ALIGNMENT BY FEEDBACK

M. Ross
Stanford Linear Accelerator Center, Stanford, CA, 94309*

Abstract
New technology is required to increase the reach of future accelerators. In keeping with several trends in technology development, new accelerator technology leads toward miniaturization and active control using high level process control systems. Linear collider designs have emphasized both and planned machines include challenging component positioning tolerances and comprehensive control systems. This paper reviews some examples of this for existing and planned linear colliders.

1. INTRODUCTION

The last decade has seen the implementation of a fundamentally new high energy particle accelerator design, the linear collider. From its conception, linear collider developers felt they could avoid the energy scaling rules associated with circular electron/positron colliders by using low emittance beams and strong interaction point focusing [1]. The SLAC Linear Collider (SLC), while not able to perform at its design luminosity, has nevertheless shown that the idea of colliding beams of very small size is feasible [2]. The salient operational accelerator issues that impact collider operation are 1) generation of intense, low emittance beams, 2) preservation of the emittance throughout accelerator and beam delivery systems and 3) stabilization over all time scales, from sub-second to hours or days.

The topic of this paper is the stabilization system, in particular the part of it that addresses mechanical components; why it is needed and what it does and what it will do in the SLC and in future linear colliders. Of course, application of beam based feedback is not new nor is its future application limited to linear colliders. Machines such as 3rd and 4th generation synchrotron light sources benefit from the use of automatic beam-based-steering feedback and component alignment schemes.

In this paper we first review linear collider tolerances, justify them and outline some of the observable signals where their impact may be seen. Following that we describe the function, design and implementation of feedback systems at SLC. In section 4 we describe experience at SLAC with SLC and outline some of the benefits of the feedback systems in use there. In the final section we describe plans for the implementation of feedback and related procedures for the Next Linear Collider (NLC) [3]. Most of the material on the SLAC based NLC design was taken from the NLC Zeroth-Order Design Report, issued in July 1996.

Stabilization is required over all practical time scales. However, in a well designed system, the more cumbersome disturbances should occur at a relatively low rate. A good example of a problem that is cumbersome to compensate for is a poorly localized, global

---

* Work supported by the Department of Energy, contract DE-AC03-76SF00515

error. Typical disturbance sources, ranging from fast to longer time scales, are shown in the Table 1.

Most linear collider designs propose operation in the range of 100 to 2000 Hz. This paper describes approaches to controlling the effects of instabilities 2–4 in Table 1 which have time scales longer than the interpulse time.

Table 1

Typical Linear Collider instability timescales, their sources and their associated feedback basis

	Timescale	Typical source	Feedback sensor/corrector
1	Pulse to pulse (collider repetition rate)	Beam dynamics, pulsed devices	Feedforward
2	Fast (few Hz)	Vibration, power converter	Position monitor/steering
3	Slow (minutes ~ hours)	Thermal	Position monitor analysis
4	Very slow (days ~ months)	Ground 'settling'	Procedure-based optimization

2. LINEAR COLLIDER TOLERANCES

2.1 Design guidelines

Linear colliders are expected to provide the next level of e+/e- collisions with energies substantially beyond what can be achieved using storage rings, albeit at the cost of some complexity and loss of stability. Several linear collider designs are quite mature [4, 5] and vary somewhat but all have: 1) a low emittance source of e+/e-, usually including damping rings, 2) long linacs and 3) final focus systems on either side of a particle detector. A critical design consideration is the preservation of emittance throughout the transport from the source to the linac, the linac itself, and the final focus. Typical normalized emittances are $\gamma\varepsilon_x = 4 \times 10^{-6}$ and $\gamma\varepsilon_y = 4\times10^{-8}$ m-rad at the beginning of the linac. In most designs, the beams at the interaction point (IP) are so small that feedback of several sorts is required for optimum performance.

Linear collider tolerances are derived from considerations of the impact that a given error has on the luminosity. As design tolerances are tightened with respect to available technology, an engineering tradeoff decision is made that separates the expected mechanical or electronic system performance, in the absence of any beam pulses, and the system performance that results from the added use of beam-based optimization schemes. In general, since there are usually observable effects associated with a particular kind of error, the performance with the inclusion of a beam-based compensation scheme is usually better and such schemes must be devised. A notable exception to this paradigm is the correction of errors that cannot be cleanly localized.

The widespread implementation of beam based tuning and optimization processes comes at some cost and can have a negative impact on the performance of the accelerator. A procedure may, in general, take time and disturb the beams substantially. Each procedure must therefore be evaluated in order to estimate how often and to what accuracy the compensation scheme must be implemented. Instrumentation accuracy, control system

latency and procedure development therefore play a vital role in the ultimate analysis of machine performance [6]. The system designers must ensure that the more complex, more difficult to correct errors need attention less frequently. In general this means that system designers must play the role of operators long before construction, not to speak of operation, begins.

Some of the most difficult errors arise in the main linac and final focus collider sub-systems. In this paper we focus on examples from those areas in both SLC and NLC. In the linac and final focus, alignment and field magnitude errors can cause significant emittance dilution or effective spot size increase as well as simple trajectory distortions. In an ideal system, the beam size would be known throughout the machine on each pulse and identification of errors would be relatively simple. In practice, the distribution of beam size monitors and their performance is somewhat limited. Thus most beam based feedback uses beam position monitors (BPM's). BPM's are distributed in great numbers throughout the LC and the ultimate ability of the feedback system to suppress long term instabilities depends critically on them. As is discussed in section 5, one of the biggest challenges for NLC feedback is the BPM offset and calibration control.

Table 2 shows some typical beam sizes and emittances associated with high energy colliders. The sizes shown for SLC are the achieved sizes during routine, nominal, operation. Design sizes are somewhat smaller.

Table 2
Typical collider (LC) beam sizes

	x (μm)	**y (μm)**
SLC linac	100	50
SLC IP	2	1
NLC - linac entrance	30	5
NLC - linac exit	15	1
NLC IP	0.270	0.005
LEP [7]	135	5

2.2 Final focus

The goal of the final focus is to demagnify the beam size by a factor of 10 to 100. One of its most critical components is the chromatic correction system (CCS) that compensates for the chromaticity of the final lens system. Typical sextupole strengths are quite large in the CCS, with pole tip fields around 5 kG and β functions with peaks close 200 km in the NLC design. The sextupoles can cause large geometric aberrations if not properly compensated.

Consider the position tolerances of the final focus quadrupoles near the interaction point (IP). On a pulse to pulse basis, the beams must remain in collision, so trajectory errors caused by the displacement of the final magnets must not result in IP motion comparable to a small fraction of the beam size. Since the beam size is quite small, the sensitivity is great. The magnet motion $\bullet y$ required to move the beam by its size (σ_y) at the IP is:

$$\Delta y = \frac{1}{k \sin \mu} \sqrt{\frac{\varepsilon}{\beta}} \tag{1}$$

where k is the inverse focal length of the magnet, μ is the phase advance to the IP, β is the beta function inside the magnet in question and ε is the beam emittance. At the SLC, $k \sim 1\ m^{-1}$, $\varepsilon = 5 \times 10^{-10}$ m-rad. and β is 10 km, giving a $\bullet y$ of roughly 200 nm. Movements much smaller than σ_y have a significant impact on luminosity so the engineering tolerance on the support stability is tighter. While obtaining stability at this level is well within the state of the art of mechanical supports, it is not trivial and some effort must be expended. The error caused by a displacement is simply an offset and no further aberrations result. This tolerance therefore must be met for short time duration only, comparable to the time between pulses. Fast, but relatively simple, IP steering feedback can be used to correct it [8]. If the correction dipoles are close by, the feedback effectively aligns the quadrupole centers. In section 4.2 this feedback is discussed further.

The principle of operation of the CCS relies on the cancellation of geometric aberrations that result from sextupoles used in the chromatic correction. This cancellation is done using a focusing cell of exactly 180$\bullet$ β phase advance between two places of equal dispersion. This cell is known as a '-I transform'.

The CCS is much more sensitive to errors generated within it than it is to incoming launch errors. With the '-I' symmetry, incoming trajectory effects are canceled. Incoming energy errors are compensated by the sextupoles. This is after all the purpose of the CCS and by correcting the aberrations caused by the energy spread of a single pulse it can, if stable, also correct for the aberrations caused by energy differences between successive pulses.

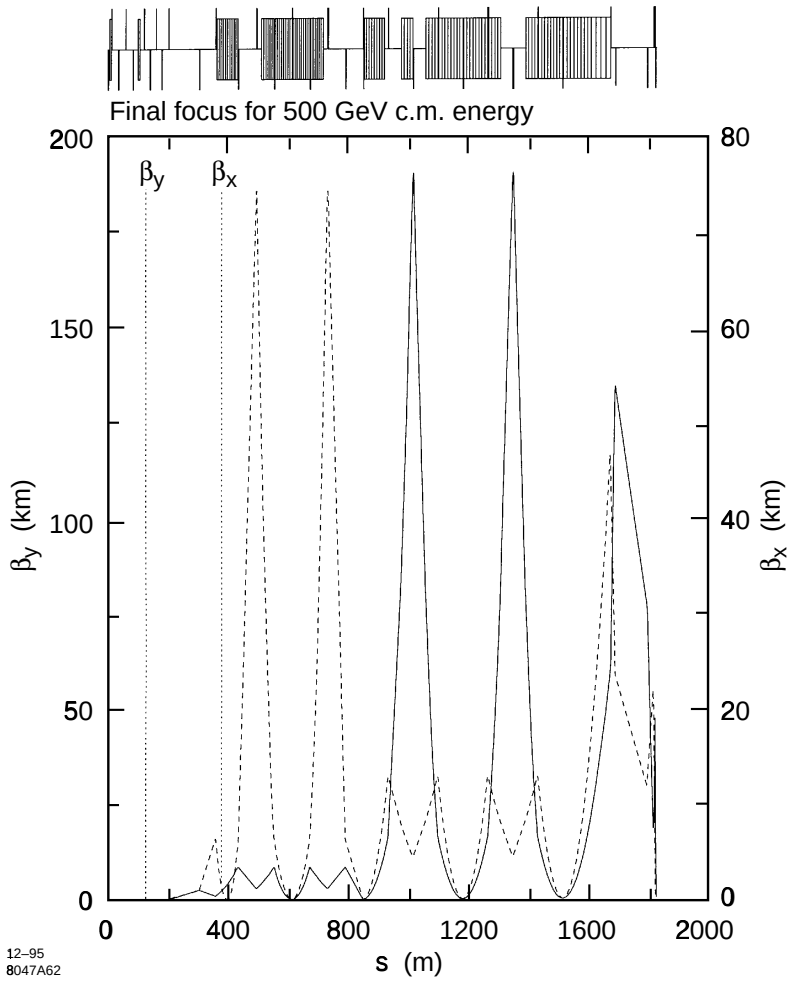

Fig. 1 NLC final focus optics. Solid line - βy , dashed - βx .

Single sextupole positioning errors generate a residual quadrupole error that can destroy the -I transform inside the CCS. Trajectory errors generated within the CCS (by, for example, correction dipoles) can have the same impact and must also be carefully controlled. Quadrupole position errors have a similar effect through their steering. Typical positioning errors for NLC are shown in Table 3. The most significant symptom of the loss of the -I inside the CCS is residual dispersion at the IP. Waist motion follows closely behind that. Typical waist shift sensitivity at SLC is 5 mm of motion for 100 μm of sextupole displacement. Since each error is evaluated on a single magnet basis, the displacement that causes a 1% luminosity loss is listed. When all magnets are taken together, the impact is more significant.

Table 3
CCS focusing magnet position errors in NLC

Magnet	**•*y* (nm)**	**Leading Error**
CCY quad	20	Dispersion
Final transformer quad	6	Dispersion

The examples given above show what some typical positioning errors can do to the performance of the final focus. In order to understand the response to systematic motion, for example, to seismic plane waves or a distortion of that nature, a formalism has been developed [9, 3] that uses the 2 dimensional power spectral density of ground motion, $P(\omega,k)$ and a lattice response function $G(k)$. The lattice response function is the normalized beam motion at the IP for quadrupole motion caused by seismic plane waves with wave number *k*. When combined with the spectral density of the ground motion ($P(\omega,k)$ or $P(k)$ for a given instant in time), the rms beam movement at the IP, $< \Delta y_B(t) >$, is given by the product integrated over seismic waves of all wave numbers:

$$< \Delta y_B(t) >^2 = \int_0^\infty P(k)G(k)\frac{dk}{2\pi} \qquad (2)$$

$G(k)$ is expected to be large for wavenumbers that are consistent with typical sizes in the beamline layout. Figure 2 shows $G(k)$ for the NLC final focus. The extremes are of special interest. In the limit of very long waves, the whole system is moved or tilted together so the sensitivity $G(k)$ is quite small. As the waves become short enough to fit between major focusing elements the response is quite large and shows the amplification expected from the demagnifying system as illustrated in Eq. (1). At this end of the spectrum, the beamline components are moving more or less independently, in a manner quite similar to the movement caused by support vibration. Note that $G(k)$ is defined here only for perfect supports that are located directly under each magnet's center. The analysis is concerned only with magnet motion associated with the plane waves. The up and down spikes in $G(k)$ arise from accidental coherence between magnets.

For given expected σ_y , positioning precision requirements may be evaluated using $P(\omega,k)$ and $G(k)$. Figure 3 shows $P(f)$ for a 'quiet' NLC final focus site. In the figure, *f* is exchanged for *k* using a dispersion relation measured at SLAC. The three curves show the

ground motion, $P(f)$, (long dash), the feedback driven damping, *F(f)*, (short dash, see Fig. 3) and the lattice response function, $G(f)$. Luckily, the effects of ground motion are strongly suppressed by the lattice response, there is little power at high frequencies. However, feedback is still required for actual physical sites, where cultural and engineering related noise sources inject significant amounts of high frequency motion. SLC experiences with such noise sources are described in section 4.

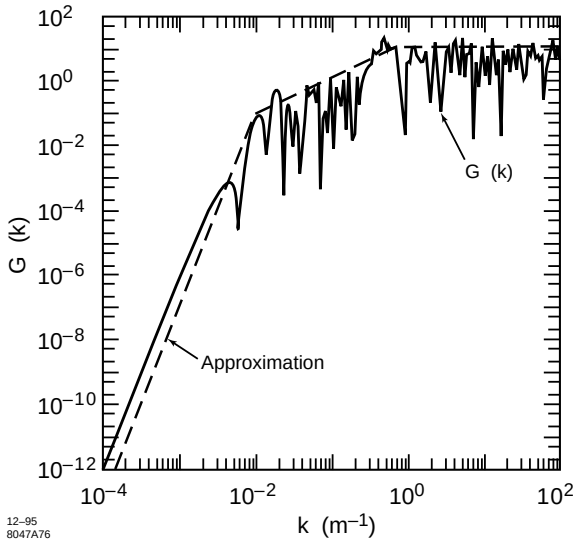

Fig. 2 Lattice response function for NLC final focus

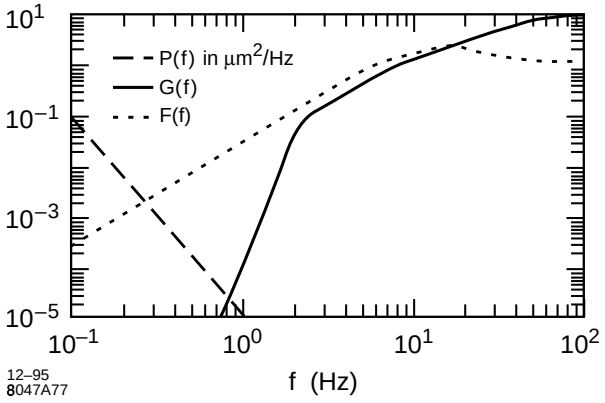

Fig. 3 Seismic plane wave spectrum for quiet site, lattice response and the expected feedback suppression ratio.

2.3 Linac

In the linac, the most challenging goal is the preservation of the beam's transverse emittance given reasonably achievable magnet and structure positioning tolerances. The NLC linac emittance growth is expected to be about a factor of 2.

The NLC linac is expected to cause about a factor of two growth in the vertical emittance. The most serious contributors to this are: 1) Transverse wakefields from beam interactions with the structure, 2) Dispersion and chromatic effects from the large energy spread beam and 3) Transverse pulse to pulse fluctuations (jitter) caused by quadrupole vibrations. Of these three, the first and last will concern us here because they will be to some extent addressed using high level automated tuning procedures and beam based feedback.

Tolerances for the linac can be derived from the same considerations of beam to beam targeting at the IP. Because of the longer, more periodic structure, $G(k)$ is larger. Alignment of the linac is critical because of the emittance growth that results from offset passage through the accelerating structures. Linac structure and quadrupole placement tolerances for NLC are shown in Figs. 4 and 5. The errors shown result in a 25% growth of ε_y. In the linac, because of its length, great care must be taken to avoid systematic misplacements of the quads and structures with characteristic length scales similar to the β function. This is the reason for the tight tolerances with $\lambda \sim 100$ m.

In contrast, the SLC structure placement tolerances are about 20 times looser because ε_y is 200 times larger. The NLC linac requires active quadrupole and structure movers for optimum performance.

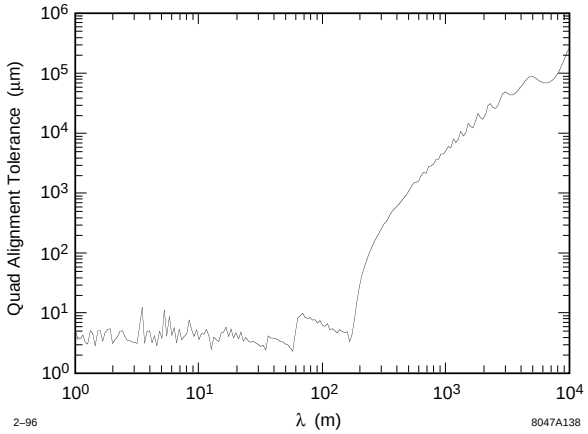

Fig. 4 NLC linac quadrupole placement tolerances vs. wavelength.

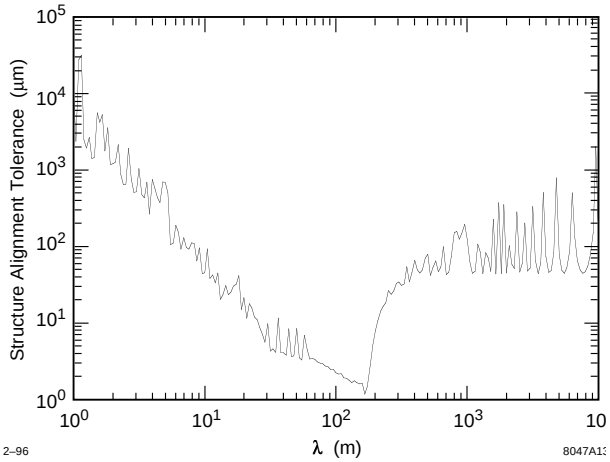

Fig. 5 NLC linac structure placement tolerance vs. wavelength

3. FEEDBACK

3.1 Goal

The goal of feedback is to stabilize steering and other beam parameters such as energy, energy spread and phase space volume and orientation using information from beam monitors. It should do this at as high a rate as possible, without decreasing stability (increasing rms beam motion), up to the beam repetition rate. Feedback also should respond quickly to step changes. The latter goal can greatly reduce the moment to moment activities of control room operators.

Typically, a feedback loop will acquire data from a given set of instruments, process it in a local processor using a filter algorithm and apply corrections through a set of actuators. Some loops do not need the response time afforded by the local signal processing and can use a simpler, slower, workstation based system. In practice exception handling and other data checks and diagnostics dominate the effort required for the implementation of the loop.

Feedback loops that include beam derived information have been used in many applications in accelerators. Typical applications are used to stabilize microwave systems, control longitudinal and transverse coupled bunch instabilities or provide local steering for synchrotron light beamlines [10]. Microwave system feedback keeps the accelerating vector in a microwave cavity oriented properly through transients seen in a variety of conditions, such as injection. This type of feedback could be considered part of that subsystem. The last example of feedback is the servo-steering used in synchrotron light machines to stabilize the light using photon beam position monitors. This feedback is responding to thermal, mechanical and other instabilities and its goal is typical of the type of loop used in linear colliders. Synchrotron light source trajectory feedback typically has a much higher response bandwidth since it involves storage rings rather than pulsed linacs. Its function is similar to the steering stabilization feedback used in linear colliders. We will not discuss the first two types of feedback since they have little to do with component alignment.

3.2 Design

Feedback at linear colliders is applied as a control layer on top of cooling water, air temperature and power converter control loops that do not nominally include beam based information.

From the point of view of the high level controls, the feedback we will describe is a digital process control loop implemented to compensate for a particular instability. In former times an operator may have been able to perform this task, but now, because the number of such tasks and the complexity of the accelerator system has grown significantly, it is imperative to relegate the task to a process control machine and do the feedback cybernetically.

The internal design of the SLC feedback loops follows somewhat formal lines [11,12]. This was done because its application was anticipated in a wide variety of situations. The design follows the 'state space' formalism adopted by digital control engineers. The state space formalism complements classical digital control design techniques that use transforms. In practice the state space formalism is better suited to multi-input – multi-output control tasks, as most beam steering applications turn out to be. Results from application of the two techniques are identical.

The beam 'state' is conveniently defined to have some meaning in the abstract, and is not directly tied to the reading of an individual monitor. Examples of 'states' are the beam energy at the end of the linac and the angle and offset of the beam trajectory at an arbitrary location in the beam line. Data from BPM's are processed through a matrix transformation and an overconstrained least squares linear fit to provide estimates of the states, which can almost never be measured directly.

The beam state information from the feedback process is used offline in accelerator modeling to interpret instabilities and other effects. It is thus a good way to connect the feedback to the bulk of the accelerator control.

The state space formalism breaks the job into two parts, the definition of a 'control law' and the evaluation of a 'state estimator'. A generic control law that calculates actuator settings from a given input state and reference is:

$$\mathbf{u}_{k+1} = \mathbf{K}\hat{\mathbf{x}}_{k+1} + \mathbf{N}\mathbf{r} \tag{3}$$

where:

u is the vector of actuator settings to be used

$\hat{\mathbf{x}}_k$ is the estimated state on pulse number *k*, ($\mathbf{x}_k$ is the actual state),

r is the reference input. In accelerator examples it is often the difference between the nominal reference trajectory and the desired trajectory.

K is the gain matrix. It contains information about the response of the system and it also contains the results of an offline optimization of the response of the loop system to the beam noise conditions.

N is the translation from **r** to actuators.

The system is managed using the knowledge of the evolution of the last known estimated state, $\Phi\hat{\mathbf{x}}_k$, the expected response from the motion of the actuators, $\Gamma\mathbf{u}$, (for example dipole correctors in many cases) and the filtered difference between the last state and the present measurement, $\mathbf{L}(\mathbf{y} - \mathbf{H}\hat{\mathbf{x}}_k)$. These terms are summed to give the new expected state, $\hat{\mathbf{x}}_{k+1}$,

$$\hat{\mathbf{x}}_{k+1} = \Phi\hat{\mathbf{x}}_k + \Gamma\mathbf{u} + \mathbf{L}(\mathbf{y} - \mathbf{H}\hat{\mathbf{x}}_k) \tag{4}$$

Φ is computed from the expected time response function of the actuators so that $\Phi\hat{\mathbf{x}}_k$ represents what has happened due to the last correction, Γ is mapping from the actuators **u** to the beam state, **L** is the optimum filter function and depends on the time structure of the instability that is to be controlled. **H** is also derived from the accelerator optics, like Γ.

Figure 6 shows the feedback processing schematic. The present actuator settings are used by a model of the machine to predict the new state, $\bar{\mathbf{x}}_k$. The difference between the predicted and observed measurements $(\mathbf{y}_k - \bar{\mathbf{y}}_k)$ is used to generate the new estimated state, $\hat{\mathbf{x}}_{k+1}$, using Eq. (4). The result is then used in Eq. (3) to determine the next correction.

Feedback needs several sorts of calibrations. First, the time response function of the correctors must be measured. Figure 7 shows the response of some typical SLC correctors. In practice, the most serious source of corrector delay at SLC is the field penetration time through the accelerator structure (~0.8cm copper). Following that, the beam transfer functions must be measured using simple corrector - BPM response tests. Finally, the expected BPM noise must be included in **L** since this is the primary source of error in the estimated state. Errors in one or more of these calibrations will result in poorer than optimum performance of the feedback system.

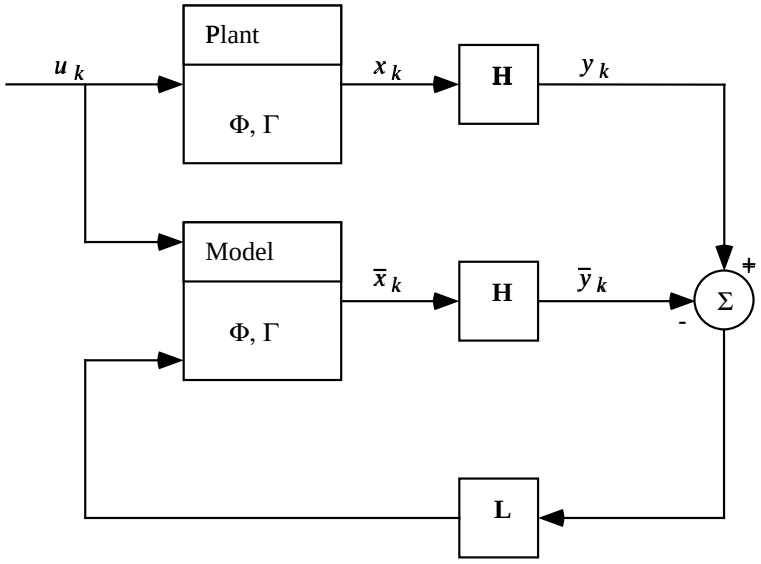

Fig. 6 Feedback system schematic

3.3 Non-linear feedback

The above examples of steering feedback are strictly linear and involve just the transfer matrices between beam line components. Non-linear feedback at linear colliders has the additional goal of automating optimization, a task usually performed by operators. Even with the application of trajectory control feedback, there remain local errors as well as the effects of accumulated global errors that require correction. An example of this is the correction of the trajectory in the linac. While the feedback provides a fixed trajectory downstream, in the region between one loop and the next upstream loop and within the region spanned by the feedback's own hardware some trajectory error occurs and can cause some degradation in the beam emittance. This has to be addressed by a global emittance correction process.

Another example appears in the final focus where systematic changes in position can cause an IP waist shift or other aberrations. The waist shift or dispersion error is not

correctable with simple steering since, after correction by the IP steering feedback, the beam remains out of optimum focus. In general, the waist can move in either direction and, unless there is some external information, a test must be done by the feedback controller to determine which direction to move [13]. What is required is a trial excursion in one direction, in order to determine the sign of the derivative of the response. Synchronous detection of the excitation allows it to be small compared to nominal operating tolerances of the device. At SLC this is known as 'dither feedback' and is under development.

Dither feedback is intended to operate on the driven derivative of the beam parameters with respect to some excitation. Since most optimization curves are locally parabolic near the optimum, the derivative is expected to be linear.

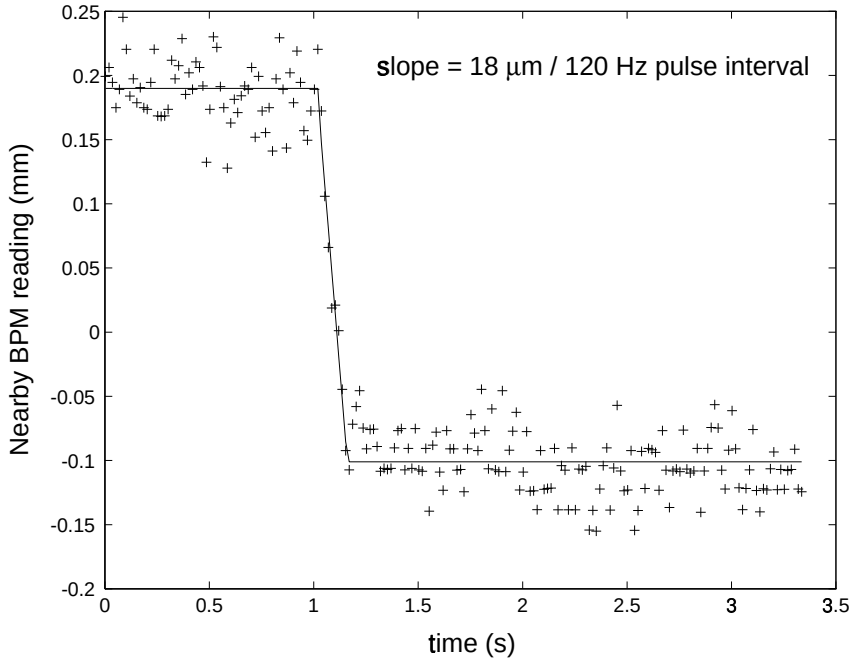

Fig. 7 Beam position monitor (BPM) response to a step change in a correction dipole. The dipole is mounted over the linac accelerating structure. The data point spacing is 1/60 s giving a dB/dt ~ 30 Gm/sec.

4. EXPERIENCE AT SLC WITH FEEDBACK

4.1 Design

Feedback loops can develop as part of the system design, as in NLC, or they can be developed in response to an observed problem. There is a set of steps through which a given procedure evolves as it passes from development to routine to automated use. This is mirrored in manufacturing when a prototype is brought into mass production. It is typical of feedback's application to the prototype collider, SLC.

The noise structure of the SLC beam (jitter) contains a large amount of broadband 'white noise', a significant component at low frequencies, corresponding to thermal time scales, and a few spikes at mechanical resonance frequencies in some cases. The feedback will easily suppress the low frequency part of this noise distribution, but its effects on the rest of the spectrum must be tuned.

Figure 8 shows the results of that tuning. The suppression is excellent for low frequencies, below about 0.5 Hz, and poor for higher frequencies. There is a region where some anti-damping is observed. Since a large part of the beam rms comes from the low end of the jitter spectrum, this design satisfies the two fold goal of reducing the jitter and providing excellent response to step changes. It is hard to reduce the anti-damping and it can lead to problems, especially if the beam motion is driven by support vibration in this frequency range.

The plot shows the rejection ratio as a function of excitation frequency. The disagreement between the model and the measured feedback response is due the variations in correction magnet slewing times. The figure shows the simulated response (smooth curve), data obtained from transforming step impulses (jagged line) and data obtained from transforming cyclic excitations at various frequencies (black dots). The step response data is more sensitive to BPM noise since only a handful of steps were used. The frequency domain data is much cleaner since more averaging could be done.

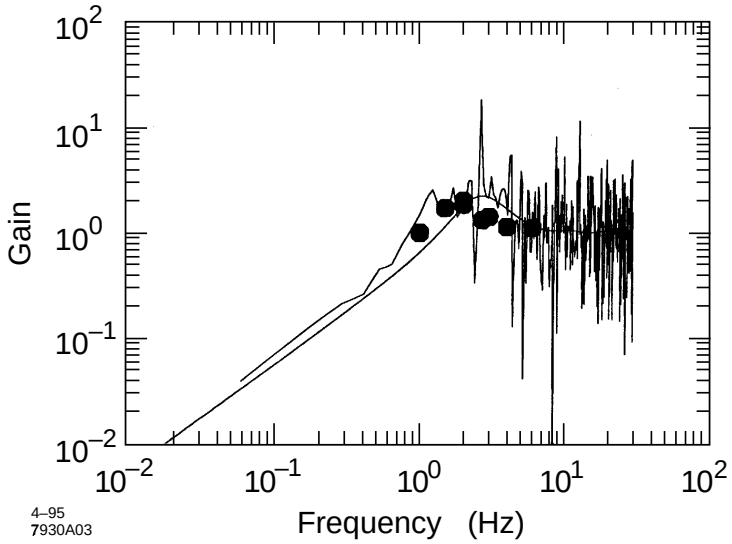

Fig. 8 Measured and simulated frequency response for an operating SLC feedback loop

4.2 Examples

Seventy percent of the feedback loops at SLC control local beam orbit steering. Typically, a group of 6 to 8 BPM's, spread over 4 linac FODO focusing cells with ~70• β phase advance, are used in conjunction with a pair of dipole correctors in each plane. The dipole correctors, spaced by roughly 90• β phase advance, are usually upstream of the BPM's so that their behavior is checked by the measurement vector **y**. Each such linac loop provides independent *x, x', y* and *y'* control for both e+ and e- beams. About 30 such loops are routinely used in SLC operation and have proven vital for operation, often in ways beyond simple stabilization of beam jitter and drift.

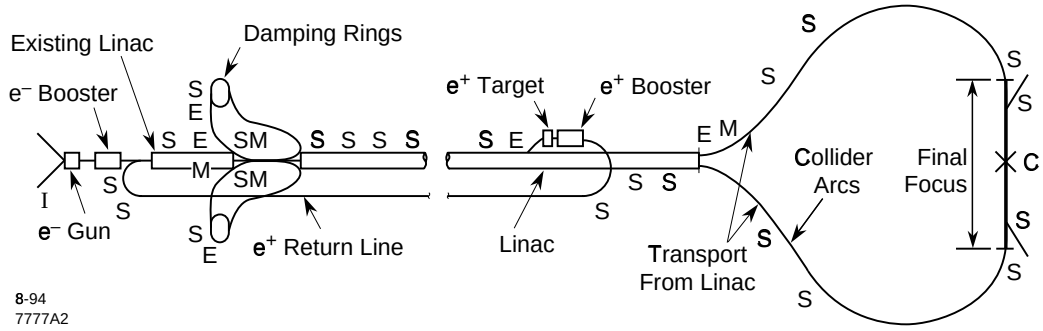

Fig. 9 Feedback installations at SLC. The figure shows a schematic of SLC with a code to indicate the function of the digital feedback loop at that location:
S - steering, E - energy, I - intensity, C - collision, M - minimization (dither feedback).

An example of a special purpose feedback loop at SLC is the IP collision steering feedback which uses a key effect seen at linear colliders, the beam-beam deflection [14]. The instrumentation used for the feedback are the two pairs of BPM's for each beam (a total of 8) used to determine the incoming and outgoing path along the ± 8 m near the IP. The BPM's are located in the IP focusing triplet structure. Information from the incoming BPM's is vital for two reasons: 1) typical beam pulse to pulse fluctuations are arbitrary in phase of origin and equivalent to about 20% of the $\sigma_{y,y'}$, the spatial and angular size of the beam, and 2) $\sigma_{y'}$, the size of the beam's angular divergence at the IP is around 300 μrad, about the same order of magnitude as the observed deflection. Indeed, additional incoming trajectory information is needed to further constrain the fit and give more accurate results.

Figure 10 shows the beam-beam deflection at SLC. In this plot, the kink angle caused by the effect of one beam on the other is plotted vs the steering of one of the beams. To take the data, the steering is accomplished in a quick succession of pulses. The plot shows a fit to the expected deflection function. The fitted parameter Σ_y shows the convolution of the two beam's vertical sizes, 0.584 μm. The fit does not provide information about the individual σ_y, in this case it is estimated from measurements using more conventional size monitors.

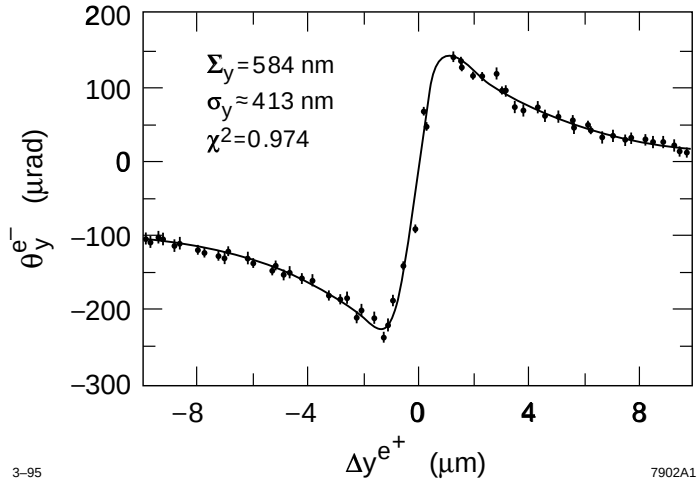

Fig. 10 Beam-beam deflection at SLC

When the beams are right on top of each other, they are optimally in collision, and the deflection is zero. Near that point the deflection is linear as a function of offset and the slope

is a good indication of the width. Thus the feedback has a relatively simple job to do; simply apply the steering correction to one beam in proportion to the observed deflection. Since the deflection is a reflexive effect, it is not possible to determine which of the two beams has caused the error from it alone. Some care must be taken to avoid compensating the motion of one beam by moving the other.

Even at transverse separations of many times σ_{xy}, a substantial kick is clearly visible at SLC. The figure shows this clearly, with a deflection many times the intrinsic error in the measurement still visible at the edge of the plot, approximately 20 σ_y from the central region. This makes the loop quite robust and it often restore collisions quickly even after a significant time has passed or after beam steering changes have been made. This is one feature of the linear collider that compensates for some of its natural instabilities.

Table 4 summarizes the application of feedback and routine optimization in the SLC. The second column of the table indicates the type of feedback, restoration to a specific setpoint (F) or optimization, 'best' value tuning (O). Loops of types 1 and 3 have been the most successful and are described in the text. Energy feedback is quite similar to steering, and uses local spectrometer optics to estimate each pulse's energy. This type of loop is also quite successful. Other rows refer mostly to optimization, done either manually or with the aid of semi-automatic data gathering and processing tools.

Table 4

Feedback and optimization in use or planned at SLC

	Parameter Controlled	**F/O**	**Detection Instrument**	**Bandwidth max 120Hz**	**Features**
1	Position and angle	F	BPM	20 Hz	provides diagnostic data
2	Energy	F	BPM	120 Hz	
3	Collision	F	IP BPM's (deflections)	120 Hz	
4	Compressor optics	O	Wire scanners at linac launch	hours	Uses asymmetric gaussian fits
5	IP spot	O	Deflections and luminosity mon	minutes	Can use dither
6	Linac emittance	F	Wire scanners in linac	minutes	Uses asymmetric fits and skew moment propagation
7	Beam phase (linac energy spread)	F	BPM's using dither phase synchronous excitation	minutes	All pulses must be dithered to achieve needed accuracy
8	Positron capture phase	F	Beam power integrator	120 Hz	uses estimated temperature
9	Kicker timing	O	Linac BPM's	minutes	Correlates beam with kicker thyratron timing
10	Arc tuning	M	Arc BPM's	days	Highly specialized; expert based optimization

4.3 Results

Perhaps the best way to illustrate the impact of feedback on machine performance and understanding is through illustrations of 'history' or time record data from relatively long time periods. In the figures, we show examples of the kind of hints that feedback can provide that are subsequently used to guide improvement efforts.

Through history records, feedback can indicate alignment degradation and component drifts over day and week time scales. At the other end of the frequency spectrum, at very short intervals, feedback and its related data acquisition can provide data relating to mechanical vibration, another form of poor mechanical subsystem performance.

Prior to the feedback era, the operator could examine the change in trajectory with respect to the saved reference trajectory and make hand corrections to null the difference. Since the changes are relatively slow, with multi-hour time scales, this is not an unreasonable way of responding to this slow drift. However, as the number of such locations grows and as better quality is required of the nulling process, it becomes unreasonable to expect the operator to correct the trajectory in each location. The primary goal of feedback at the SLC is exactly this. Through the records kept by the feedback process, a diagnosis of the source of the drift can begin. Without feedback, with each operator correcting the drift using a slightly different technique, the clear unfolding of the underlying causes is more difficult.

Figure 11 shows a record of the beam trajectory at the exit of the SLC damping ring for a period of several days. The two 'history' records in the figure show the performance of the feedback at the exit of the electron damping ring (top) and the beam intensity (bottom) during the 10 day interval May 5, 1996 through May 15, 1996. There are about 10 data points per day with a point to point spacing of 2 hours. In the figure the points are connected. The dips shown in the bottom plot are the intervals when the beam was absent from the ring. During that time, the ring cools substantially and the components in it move a little, maybe 20 to 40 μm; the exact amount is not known. In the top plot, the correction required to keep the vertical trajectory fixed to within a 5 to 10 μm rms in the extraction transport is shown. This is actually $\Gamma\mathbf{u}$ from Eq. (4).

An interesting aspect of this plot is the movement required by the correctors to stabilize the orbit after the beam is restored. Typical decay constants are ~1 hour. One of the events is noteworthy, early in the afternoon of May 7 the response is more severe due to the de-excitation of the magnet power converters. In each of the other events, only the beam was off. To further reinforce this, note the two large corrector events late on the 13th and during the afternoon of the 14th. In these episodes the beam was present, but at a much lower duty cycle, about 15% of nominal. Thus the power dissipated in the ring by higher order mode losses in the ring's internal structures and synchrotron radiation is reduced. These two taken together amount to 25 kW for nominal, full repetition rate, operation at 9×10^{10} e- in two bunches (120 mA). The motions caused by the 'beam off' events are corrected by a 50 μrad kick, equivalent to a magnet strength of 1 to 2 Gauss-meters. The correction elements involved produce a 1 G-m kick with an excitation of 0.12A. Their tolerances are set at 10% of that.

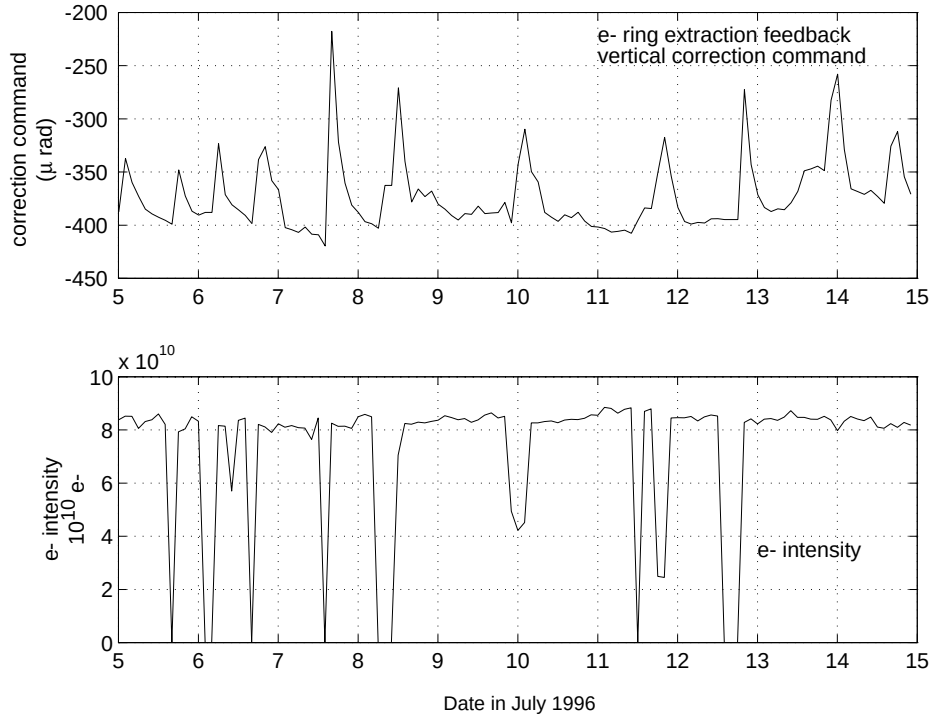

Fig. 11 Ten-day history record of extraction from the electron damping ring showing correlation with beam intensity

Figure 12 illustrates another kind of thermal instability, this one associated with the ever present day night temperature changes of the California climate. The figure shows the temperature inside the SLC final focus (solid) during a 10 day interval in July 1996 superimposed on the vertical feedback correction command (dashed). The tunnel temperature changes are small (within 2.2 •F or 1.2 •C), but they are large enough to cause the beam trajectory to move. The outside temperature is shown above the plot in order to indicate the extent to which it contributes to the apparent motion. Note the phase shift between tunnel temperature and the feedback actuator. In this example, the temperature of the outside environment is causing slight misalignments of the machine components. This can be fixed with improved environmental control and by examining the local optics sensitivity.

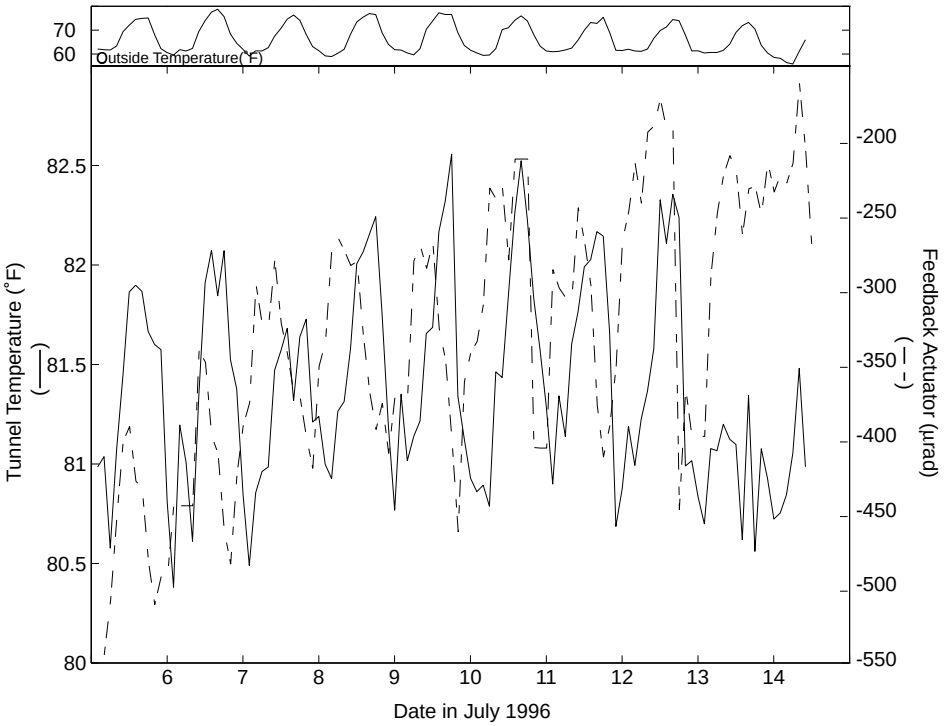

Fig. 12 Ten-day history of initial beam launch conditions in the SLC final focus showing the correlation with temperature

Figure 13 shows another result from the SLC final focus. The data was not derived from the feedback process itself, as in the other examples, but from a similarly constructed monitor or 'watchdog' process. The watchdog in this location is intended to monitor the positions of the CCS sextupoles. It does this by keeping track of the average BPM readings in the '-I' spaced sextupoles. The presence of an incoming and outgoing beam is an added feature of the final focus that adds redundancy to the monitor. The sextupole pair position illustrated in Fig. 13 exhibit roughly 100 μm peak to peak vertical day to night motion. A thermocouple mounted on the support of one of the magnets shows the temperature correlation, presumably indicating the cause of the problem.

The performance of the feedback depends on the incoming pulse fluctuation characteristics. For example, if the feedback is tuned for a broadband, smooth frequency pulse to pulse jitter spectrum with no particular single frequency lines, it will respond in a different way than if these lines were suddenly to appear with some strength. Causes for this may be associated with electronic or mechanical failures. The vertical motion spectrum of a pathological linac quadrupole is shown in figure 14. The quadrupole is pushed longitudinally at its support's resonant frequency by the water cooling the nearby accelerating structure. Normally this would have no impact on the magnet's vertical position but, in this case, the support is not directly under the magnet so the longitudinal motion is coupled into the vertical. Figure 15 shows the beam jitter spectrum in the SLC linac. Resonance lines associated with the mechanical support systems may be seen at 10 Hz. The beam size in this location is about 80μm. Using this analysis, we have been able to identify and correct various support related instability signatures in the 5 to 40 Hz range. Figures 14 and 15 show two such problems.

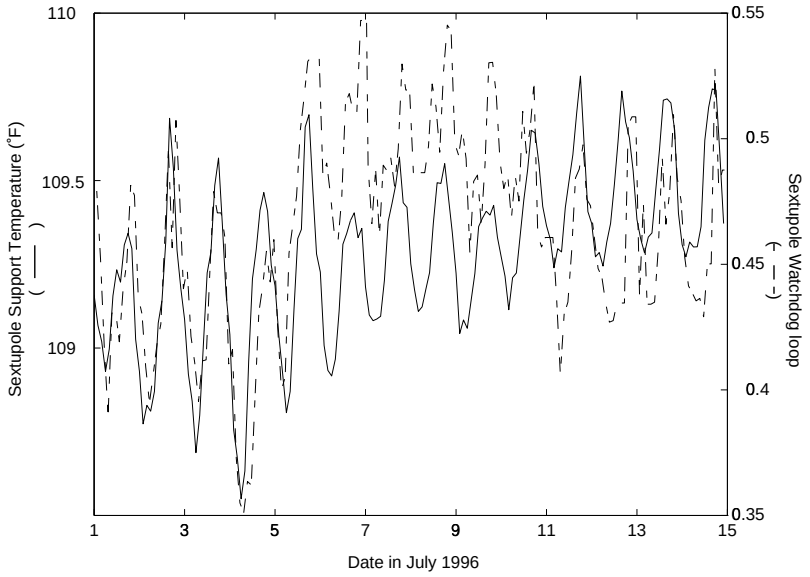

Fig. 13 15-day record from the SLC final focus sextupole positioning monitor showing the correlation with the sextupole support temperature. The units of the left side of plot are mm.

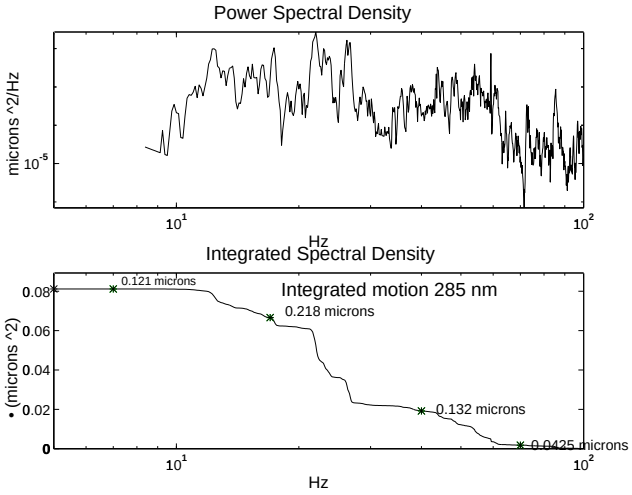

Fig. 14 SLC linac quadrupole vertical position motion spectrum

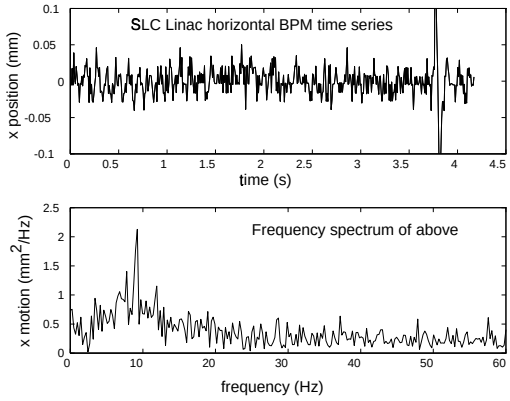

Fig. 15 SLC Linac beam jitter

In the pathological example shown in Fig. 14, the quadrupole has residual resonant behavior at 20–30 Hz. The top plot is the power spectrum from the commercial accelerometer. The bottom part of the figure shows the integral of the spectrum, starting from high frequencies. This plot shows the total amplitude of the motion in the frequency range 2–100 Hz. In this range, feedback performance is poor, but its data stream can be used to diagnose problems. The steps in the bottom plot, show by what fraction the total motion is reduced if the support is stiffened.

The BPM data shown in Fig. 15 come from a pair of digitizers per plane (x,y); the ratio of the numbers gives x or y. Since the numerator is close to zero, its bit noise is much more

significant and, in the top part of the plot, this digitization quantization is easily seen, with the least significant bit size of about 20 μm. However, the 10 Hz component of the beam motion is also clearly seen in the first section (0 - 1 s) of the top plot.

In the last example, Fig. 16 shows how feedback can be used to track jitter over long time scales. It shows the history of the pulse to pulse stability of the electrons at the entrance to the linac, integrated over about 10 seconds, for a 92 day period from May 1 to August 1. This case, also illustrating an anomalous event, the beam jitter grew in late July 1996 by about a factor of 2. The cause for this increase is not understood; typical angular beam sizes in that location are 50 μrad, so this jitter is quite small by comparison. The jitter 'floor' of about 30 nrad in the plot is caused in part by instrumental noise.

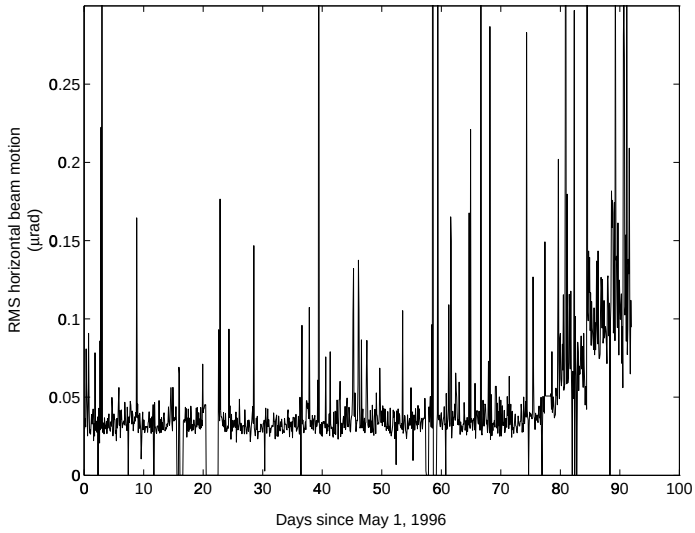

Fig. 16 Three-month history record of beam rms horizontal motion, or 'jitter', at the entrance of the linac (1.2 GeV)

5. APPLICATIONS – NEXT LINEAR COLLIDER

Widespread use of feedback systems forces a more careful look at instrumentation, particularly BPM, performance. In effect, by using BPM's as the primary sensors for feedback systems, the BPM system becomes part of the power converter control system. It is therefore critical to avoid systematic errors in the instrumentation, such as thermally dependent gains and offsets since these will compete with similar offsets arising from thermal effects in the power converters and mechanical supports.

In the NLC linac an on-line BPM offset calibration scheme must be devised for generating corrections. If a monitor system with inherent offset stability or equivalently, an accurate offset calibration system were devised, then a beam based BPM calibration scheme would not be as critical. Most BPM systems do not have an offset calibration mechanism that is part of the BPM and calibrates the monitor, cable response and electronic offsets. Reference [15] is the only one found and it includes no long-term performance data. It is anticipated one will be required at NLC. Figure 17 shows how it might work.

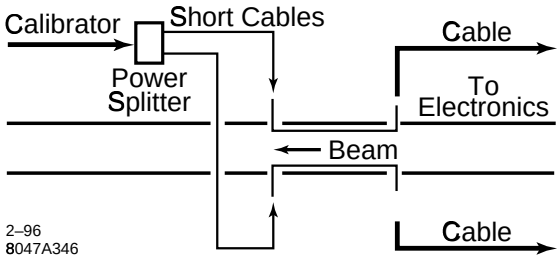

Fig. 17 NLC Linac BPM calibration

Beam based BPM calibration schemes have been tested at LEP [16] and SLC. The schemes rely on either 1) sub-tolerance excitation and synchronous detection or 2) use multiple kinds of beams, such as positrons and electrons traveling in the same direction, or beams of different energies. In most of these cases a BPM offset, arising from within the instrumentation itself is not easily distinguished from the offsets of the beam line components themselves. Since the drifts in the instrumentation are equally as severe as movements of the components themselves, automated schemes are required for finding and correcting them. The schemes, both tried and proposed, fall into two categories, invasive and non-invasive. Non-invasive is somewhat of a misnomer since the procedure may still have an impact on the luminosity. We list here three schemes.

Reference [15] is a good example of the sub-tolerance excitation referred to in section 3.3. Individual LEP quadrupole magnet windings are excited using a sine function current source with 10^{-4} strength of the nominal current. BPM zero offsets with respect to the quadrupole center are determined by watching the magnitude of the beam response to the excitation. If the offset is large, the response will be correspondingly large. Since the excitation is narrow band, in the range of 1 to 17 Hz, and the data acquisition is broadband and can provide data from each LEP turn, the signal/noise ratio is very good. Different frequencies can be used with different quadrupoles so that optimization of several can proceed at the same time. A beam pickup similar to those used for the tune measurement provides the line strength information. A local beam bump near the quadrupole in question can be varied until the transfer of the sine signal is minimized. An accuracy of about 100 μm has been achieved.

In the case of SLC linac [17] BPM's offsets can be estimated using the trajectories of the e+/e- beams in a short, three BPM section. The simple geometry is illustrated in Fig. 18. The position monitor measurements, $\vec{\mathbf{y}}_m$, can be related to the incoming position and angle of both beams and the offsets of the intermediate magnet and BPM using:

$$\vec{\mathbf{y}}_m = \mathbf{M}\vec{\mathbf{v}} + \vec{\mathbf{c}} \tag{5}$$

where

$$\vec{\mathbf{v}} = \begin{bmatrix} y_0^- \\ y_0^+ \\ \theta_0^- \\ \theta_0^+ \\ y_B \\ y_Q \end{bmatrix} \tag{6}$$

is the vector of initial conditions and the central monitor's offsets, $\vec{\mathbf{c}}$ contains adjustments associated with the small correction dipoles and **M** is the transformation matrix between these vectors. The last two elements in $\vec{\mathbf{v}}$ are the offset of Q2 with respect to the line drawn between Q1 and Q3 (y_Q) and the offset of the BPM inside Q2 with respect to its magnetic center (y_B). The latter term has contributions from the mechanical BPM electrodes, the cables connecting the BPM to the electronics and the electronics itself.

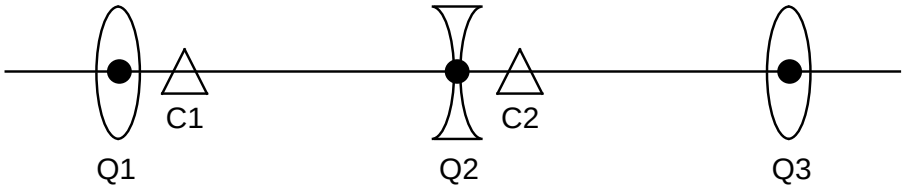

Fig. 18 SLC BPM alignment test schematic

The analysis works well where the phase advance per cell is small compared to 90• and it assumes that y_B is the same for e^+ and e^-. This is not always be appropriate since the electronics will respond differently for opposite polarity signals. It has been used to monitor offset stability.

The NLC linac will use a combination of these three calibration mechanisms. NLC linac quadrupoles are mounted on movers so that their offsets with respect to each other can be perturbed and therefore nulled. With the cam based mover mechanism [18] it is possible to move the magnets in increments small compared to the single component position tolerances. This may also work with synchronous detection techniques.

6. CONCLUSION

In the last decade, commercially available test instrumentation with integrated processing has greatly improved in performance. This is clearly illustrated in the improvements to alignment instrumentation. It is important to develop this technology and try to realize the benefit and cost saving that it affords in the next generation of accelerators. Linear colliders and free-electron laser accelerator systems are perhaps the first to require such accurate component positioning, but they probably won't be the last.

REFERENCES

[1] B. Richter, The SLAC Linear Collider: the machine, the physics, and the future, SLAC-PUB-2854, Nov. 1981, DPF 1981:433.

[2] P. Emma, The Stanford Linear Collider, SLAC-PUB-95-6866, Proceedings of 16th IEEE Particle Accelerator Conference (PAC 95) and International Conference on High Energy Accelerators, May 1995.

[3] T.O. Raubenheimer, ed., Zeroth order design report for the next linear collider, SLAC Report 474, 1996.

[4] J. Urakawa, Proceedings of the sixth international workshop on linear colliders, KEK Proceedings 95-5, August 1995.

[5] R.B. Palmer, Ann. Rev. Nucl. Part. Sci. 40: 529-592, 1990.

[6] M.C. Ross, Requirements for linear collider instrumentation, SLAC-PUB-6134, Euro. Beam Instrum. 1993: 151-155, May 1993.

[7] D. Bourilkov, et al., Beam spot position measurement at the LEP collider, Submitted to Nucl. Instrum. Methods.

[8] M.G. Minty, et al., Feedback performance at the Stanford linear collider, SLAC-PUB-95-6817, Proceedings of 16th IEEE Particle Accelerator Conference (PAC 95) and International Conference on High Energy Accelerators, Dallas, Texas, May 1995.

[9] V.M. Juravlev, et al., Investigations of power and spatial correlation characteristics of seismic vibrations in the CERN LEP tunnel for linear collider studies, CERN-SL-93-53, Dec. 1993.

[10] R. Hettel, Rev. Sci. Instrum. 60 (1989) 1501-1506.

[11] G.F. Franklin, J.D. Powell and M.L. Workman, Digital Control of Dynamic Systems, Addison Wesley (1990).

[12] T. Himel et al., SLAC-PUB-5470, Particle Accel. Conf: IEEE 1991: 1451-1453.

[13] M.C. Ross, et al., Proceedings of the IEEE PAC 1993: 1972-1974.

[14] Wayne A. Koska, et al., Nucl. Instr. Meth. A286: 32, 1990.

[15] S. Battisti, et al., 1987 Particle Accelerator Conf., PAC 1987: 605.

[16] I. Barnett et al., Dynamic beam based calibration of orbit monitors at LEP, CERN-SL-95-55-BI, June 1995. Proceedings of the 2nd European Workshop on Beam Diagnostics and Instrumentation for Particle Accelerators (DIPAC'95) 1995, - CERN-SL-95-055.

[17] This analysis was done by Chris Adolphsen.

[18] G. Bowden, et al., Nucl. Instrum. Meth. A368: 579-592, 1996.

[1] B. Richter, THE SLAC LINEAR COLLIDER: THE MACHINE, THE PHYSICS, AND THE FUTURE. SLAC-PUB-2854, Nov 1981, DPF 1981:433.
[2] P. Emma, THE STANFORD LINEAR COLLIDER, SLAC-PUB-95-6866, Proceedings of 16th IEEE Particle Accelerator Conference (PAC 95) and International Conference on High Energy Accelerators, May 1995.
[3] T. O. Raubenheimer, ed., ZEROTH ORDER DESIGN REPORT FOR THE NEXT LINEAR COLLIDER, SLAC Report 474, 1996.
[4] J. Urakawa, PROCEEDINGS OF THE SIXTH INTERNATIONAL WORKSHOP ON LINEAR COLLIDERS, KEK Proceedings 95-5, August 1995.
[5] R.B. Palmer, Ann.Rev.Nucl.Part.Sci.40:529-592,1990.
[6] M. C. Ross, REQUIREMENTS FOR LINEAR COLLIDER INSTRUMENTATION, SLAC-PUB-6134, Euro.Beam Instrum.1993:151-155, May 1993
[7] D. Bourilkov, et.al., BEAM SPOT POSITION MEASUREMENT AT THE LEP COLLIDER, Submitted to Nucl. Instrum. Methods
[8] M.G. Minty, et.al., FEEDBACK PERFORMANCE AT THE STANFORD LINEAR COLLIDER, SLAC-PUB-95-6817, Proceedings of 16th IEEE ParticleAccelerator Conference (PAC 95) and International Conference on High Energy Accelerators, Dallas, Texas, May 1995.
[9] V.M. Juravlev, et. al., INVESTIGATIONS OF POWER AND SPATIAL CORRELATION CHARACTERISTICS OF SEISMICVIBRATIONS IN THE CERN LEP TUNNEL FOR LINEAR COLLIDER STUDIES. CERN-SL-93-53,Dec 1993.
[10] R. Hettel, Rev. Sci. Instrum. 60 (1989) 1501-1506.
[11] G. F. Franklin, J. D. Powell and M. L. Workman, Digital Control of Dynamic Systems, Addison Wesley (1990).
[12] T. Himel, et.al.. SLAC-PUB-5470, Particle Accel.Conf: IEEE 1991:1451-1453.
[13] M.C. Ross, et.al., Proceedings of the IEEE PAC 1993:1972-1974.
[14] Wayne A. Koska, et. al., Nucl.Instr.Meth.A286:32,1990.
[15] S. Battisti, et.al., 1987 Particle Accelerator Conf., PAC 1987:605
[16] I. Barnett et. al., DYNAMIC BEAM BASED CALIBRATION OF ORBIT MONITORS AT LEP, CERN-SL-95-55-BI, Jun 1995. Proceedings of the 2nd European Workshop on BeamDiagnostics and Instrumentation for Particle Accelerators (DIPAC'95) 1995, - CERN-SL-95-055.
[17] This analysis was done by Chris Adolphsen
[18] G. Bowden, et.al., Nucl.Instrum.Meth.A368:579-592,1996.